Firing thyristors with negative firing angle using multilevel current reinjection concept: an experimental evaluation

Bhaba Priyo Das* and Neville Watson

Department of Electrical and Computer Engineering,
University of Canterbury,
Christchurch, New Zealand
Email: bhaba.das@pg.canterbury.ac.nz
Email: neville.watson@canterbury.ac.nz
*Corresponding author

Yonghe Liu

Department of Information Engineering,
Inner Mongolia University of Technology,
Hohhot, China
Email: yonghe.liu@canterbury.ac.nz

Abstract: Thyristor based multilevel current reinjection (MLCR) current source converter (CSC) provides self-commutation capability to thyristors. It also has high quality line current waveform by accurately shaping the DC bus current using an auxiliary reinjection bridge. However the theoretical and PSCAD/ETDC simulation analysis do not take into account the inevitable stray capacitances and inductances which may influence the thyristor turn-on/off and the simulation switching model may not represent the switching characteristics of the main bridge thyristors fully or accurately. Questions have been raised about the ability to achieve self-commutation with thyristors and the possibility of operating thyristors with negative firing angles. Therefore, it is necessary to experimentally verify whether neglecting the real-world artefacts actually impedes the performance of thyristor based MLCR CSC. The experimental results presented in this paper prove that the auxiliary reinjection circuit can force the thyristor to commutate independently from their respective line-to-line voltages and thyristor converter can operate with a negative firing angle.

Keywords: alternating current to direct current (AC-DC) conversion; firing angle; harmonics; multilevel current reinjection; self-commutation.

Reference to this paper should be made as follows: Das, B.P., Watson, N. and Liu, Y. (2015) 'Firing thyristors with negative firing angle using multilevel current reinjection concept: an experimental evaluation', *Int. J. Power Electronics*, Vol. 7, Nos. 3/4, pp.166–184.

Biographical notes: Bhaba Das received his BE in 2005 from University of Gauhati, India, MTech (Power Electronics) in 2007 and his PhD in 2014 from the University of Canterbury, New Zealand. His main research

interest is in the application of power electronics in power systems for the smart grid. He is a member of IEEE. Currently, he is involved with the Engineering Department at ETEL Transformers Ltd in the development of smart distribution transformer for the New Zealand smart grid initiative.

Neville R. Watson received the BE (Hons.) and PhD Degrees in Electrical and Electronic Engineering from the University of Canterbury, Christchurch, New Zealand. Currently, he is a Professor with the University of Canterbury. He is a Senior Member of the IEEE. His interests include power quality, and steady-state and dynamic analysis of ac/dc power systems. He has co-authored seven books, three chapters of books and approximately 200 technical papers. He is very active in professional societies and is a member of CIGRE AP C4 committee on Technical Performance, joint Australia/New Zealand standards committee EL034 on Power Quality. He has been a contributing member of various other standards and IEEE committees.

Yonghe Liu received the ME Degree in Automation from The Chinese Science Academy, Beijing, China, and the PhD Degree from the University of Canterbury, Christchurch, New Zealand. Currently, he is a Professor at Inner Mongolia University of Technology, Hohhot, China and a Researcher at the Department of Electrical Engineering, University of Canterbury, New Zealand. He is a Senior Member of the IEEE. He has published almost 100 technical papers and co-authored three books on self-commutating converters for HVDC applications.

1 Introduction

The idea of multilevel current reinjection (MLCR) was first mooted by Liu (2003). MLCR combined the advantages of direct current (DC) ripple reinjection (Baird and Arrillaga, 1980; Arrillaga et al., 1993), multilevel conversion Rodriguez, Lai and Peng (2002) and the low loss of a soft-switching technique. DC ripple reinjection produced the same effect as that of a multi-pulse transformer (Paice, 1996) leading to a reduction in harmonic content of currents and voltages both in the AC and DC-sides. DC ripple reinjection technique was one form of current injection which used rectangular reinjection currents resulting in a 24-pulse operation of a 12-pulse current source converter (CSC). The basic idea was extended to higher pulse operations (Mohan, Singh and Panigrahi, 2009; Gairola and Singh, 2011) by the addition of extra discrete steps to the injection current through extra reinjection thyristor switches or increased reactor taps. Although higher pulse numbers were achieved, this concept was 'true' mostly for pulse doubling i.e 24-pulse operation of a 12-pulse converter. This was evident from the lower order harmonics appearing in the higher pulse configurations (Villablanca, Arias and Acevedo, 2002). The reinjection waveforms were determined using phasor diagrams and graphical interpretation and the lack of mathematical explanation made the optimisation of the reinjection waveform for harmonic cancellation a difficult task.

Early developments in the DC ripple reinjection concept were based on thyristors and hence the reinjection current was dependent on the line commutation condition of the thyristor. The use of thyristors was understandable as at that time as self-commutated switches were in their early days. The continued use of thyristors meant that there was the need for reactive power support.

With the advancement in the voltage and current ratings of the self-commutated switches, self-commutated switches are beginning to replace thyristor switches. Thus the dependency on the line commutation condition could be avoided if self-commutated switches are used for DC ripple reinjection. This improved reinjection concept based on optimising the current reinjection waveform to achieve harmonic suppression is termed as the MLCR concept. The optimised reinjection current (I_{inj}) should be a triangular waveform operating at six times the fundamental frequency of the AC system (Liu, Arrillaga and Watson, 2008). The DC bus currents when modified by triangular I_{inj} showed the following characteristics (Figure 1):

- DC bus currents have zero current at points where the main bridge thyristors commutate
- both add up to a DC level with ripple.

Figure 1 The ideal DC bus waveforms for completer harmonic elimination in a 12-pulse CSC

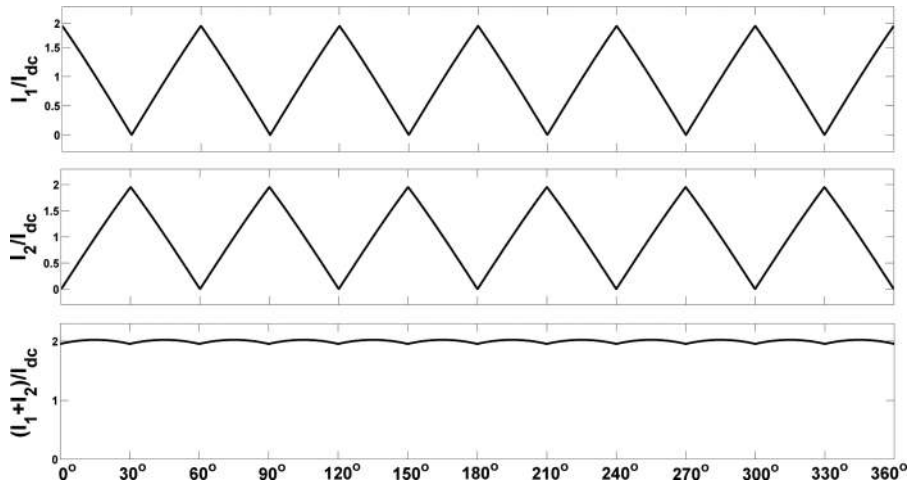

Assuming that this ideal I_{inj} can be supplied to the two bridges, the current waveforms of the 12-pulse converter are shown in Figure 2. A pure theoretical sinusoidal line current waveform is obtained (THD $= 0\%$) due to complete harmonic cancellation.

The main bridge commutation occurs at 0°, 30°, 60°, 90°, 120°, 150°, 180°, 210°, 240°, 270°, 300°, 330° and 360°. To use thyristors instead of self-commutating switches, zero current switching (ZCS) conditions are needed, before and after the main bridge commutation occurs, by controlling the magnitude and duration of I_{inj} and ensuring that the modified thyristor currents are forced to zero during the commutations

instants. For a practical thyrsitor based MLCR CSC, I_{inj} is derived as a stepped approximation (multilevel) by a multi-tapped reinjection transformer (discussed later on). This stepped reinjection waveform (linear waveform) provides true zero current periods during main bridge commutation periods as shown in Figure 3.

Figure 2 Current waveforms of 12-pulse CSC with ideal reinjection

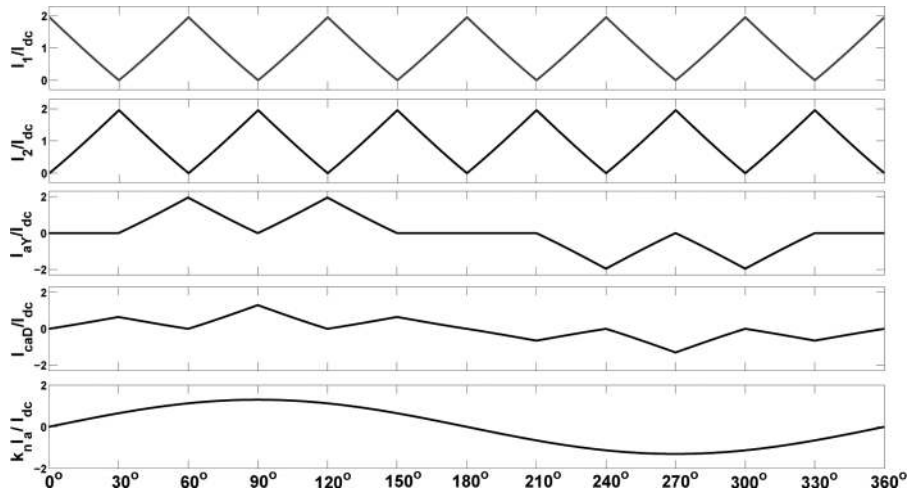

Figure 3 Stepped DC bus current waveform approximating linear reinjection

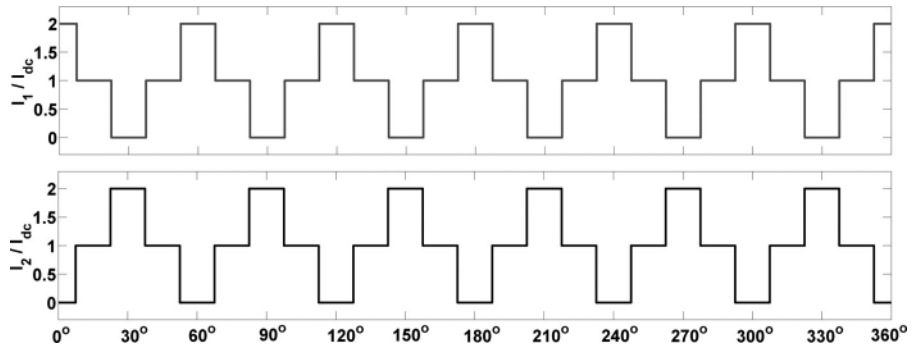

With controllable ZCS (achieved by controlling the width and height of the multilevel reinjection steps using the reinjection bridge), self-commutation is added to a thyristor converter. Thyristor based MLCR CSC was introduced in Arrillaga et al. (2006). Based on this concept, various thyristor based MLCR CSC schemes have been proposed:

- A STATCOM where the MLCR CSC operates as a statcom under symmetrical and asymmetrical line voltages achieving fast dynamic response to system changes (Liu et al., 2006).

- A back-to-back (BTB) HVDC link where BTB MLCR HVDC with parallel connected 12-pulse bridge converter operates satisfactorily with varying active and reactive power operating conditions (Liu et al., 2007a).
- A standard HVDC link where MLCR HVDC scheme with the standard 12-pulse bridge converter operates with the same waveform quality and control flexibility of PWM-VSC schemes (Liu et al., 2007b).
- A superconducting magnetic energy storage (SMES) where series connected paralleled MLCR CSC are used to achieve four quadrant control (Murray et al., 2009).

However, the theoretical and PSCAD/ETDC simulation analysis presented so far does not take into account the inevitable stray capacitances and inductances which may influence the thyristor turn-on/off and the simulation switching model may not represent the switching characteristics of the main bridge thyristors fully or accurately. In particular, the ability to force the thyristors off using the reinjection bridge despite finite turn-off times of thyristors have been questioned. Therefore it is important to verify that neglecting some of these real-world artefacts will not impede the operation of a practical thyristor based MLCR CSC. The use of controllable ZCS duration has an important implication that the thyristors do not need to rely on the line voltage to commutate. This experimental results presented in this paper answerers the following questions:

- Is self-commutation capability achievable in a practical 12-pulse thyristor bridge despite finite thyristor turn-off times?
- Can thyristors be fired with a negative firing angle i.e line current leads the respective voltage?
- Is the probability of commutation failure reduced in a 12-pulse thyristor bridge?
- What is the actual THD reduction obtained?

To answer the above questions, a hardware prototype was designed and implemented in the laboratory. The rest of the paper is organised as follows: Section 2 briefly presents the concept of firing thyristors with negative firing angle, Section 3 details the three-level thyristor based MLCR CSC with theoretical results and Section 4 shows the results obtained from the hardware.

2 Thyristors with negative firing angles

For a conventional thyristor based converter, it is well known how the firing angle (α) is measured, giving it an effective range of $0^\circ \leq \alpha \leq 180^\circ$, (Kimbark, 1971). For a conventional thyristor based converter, if the gate current pulse is provided at a negative α, the outcome depends on the width of the gate current pulse. If pulse width is greater than the magnitude of α, it effectively means the gate pulse is being applied when incoming phase voltage is positive and the current transfer occurs at $\alpha = 0^\circ$. If the width of the pulse is less than α, commutation between the phases will not occur.

This effectively means $\alpha = 0°$ is the lower limit. Similarly, if $\alpha = 180°$, commutation voltage is zero and current continues to flow through the same thyristor. Therefore, for successful commutation, $\alpha < 180°$.

Figure 4 shows the three-level thyristor-based MLCR CSC along with the reinjection circuit. The linear reinjection approximation is utilised here to allow the use of thyristors in the main bridge of the 12-pulse converter. When a particular thyristor in the positive DC bus is triggered, the corresponding DC bus current I_1 is forced to be zero and none of the thyristors connected to the positive DC bus conduct (Figure 5). During this time, the DC current I_{dc} flows through the auxiliary reinjection path. The DC bus current I_1 is zero during commutation, due to forced clamping using the auxiliary bridge, it is possible to force turn-off the main bridge thyristors independently from their respective line voltages. The thyristor based MLCR CSC takes advantage of this modification and is able to achieve self-commutation as well as the ability to fire the main bridge thyristor with a negative firing angle ($-\alpha$), i.e., thyristor Y1 of the Y-Y connected bridge is fired at an angle α ahead of the crossing point of V_{an} and V_{cn} in their positive half cycles (Figure 5).

Figure 4 Three-level thyristor-based MLCR CSC with linear reinjection (see online version for colours)

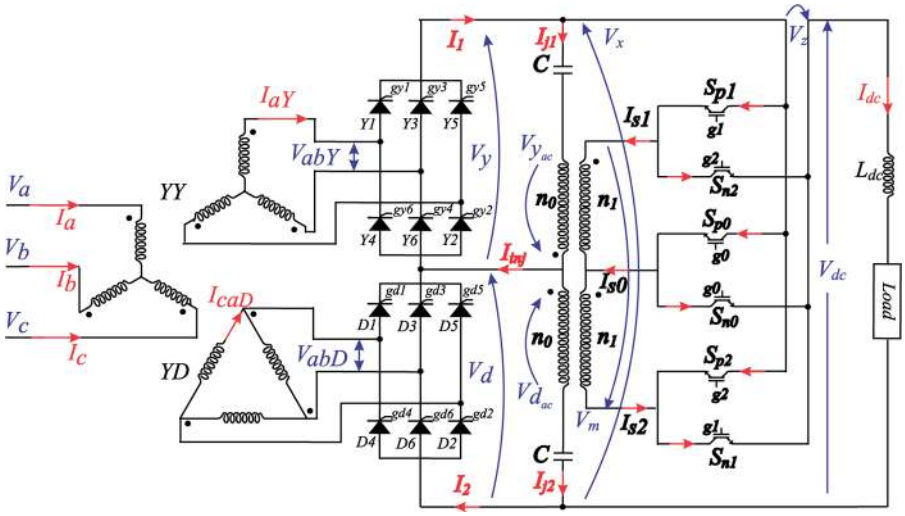

The current through thyristor Y1 of the Y-Y connected bridge (I_{Y1}) is shown in Figure 5. The gate pulse for Y1 (gY1) is applied at $\alpha = -45°$ and the current I_{Y1} flows through Y1 after 7.5° of applying gY1. This is controlled by forced current clamping using the reinjection bridge. The angular sequence for the reinjection firing sequence (repeats every $\frac{\pi}{6}$ radians) is:

$$\beta_i = \frac{(2i-1)\pi}{24}, \quad \text{where} \quad i = 1, 2. \tag{1}$$

Figure 5 Negative firing angle waveforms for a three-level thyristor based MLCR CSC

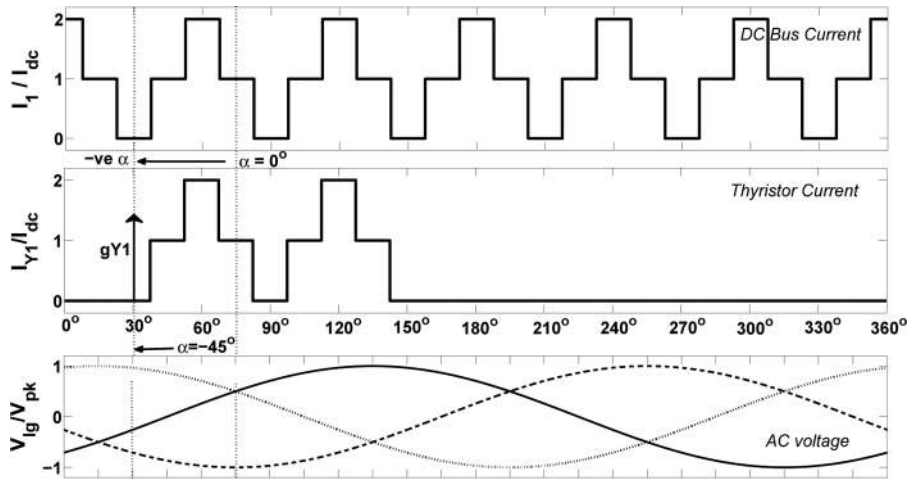

Figure 6 Firing pattern for three-level MLCR CSC (see online version for colours)

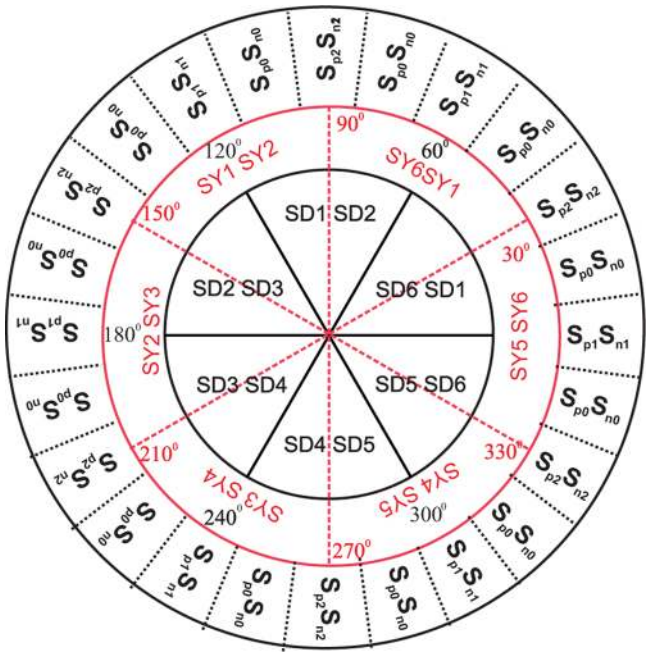

In order to achieve forced current clamping, the firing sequence of the reinjection switches are synchronised with the main thyristor bridge switching. For a 3-level MLCR CSC, the firing pattern is shown in Figure 6. The outer most circle representing the reinjection switch firing sequence is divided into 24 sectors. The 12 zero current

intervals of the three-level reinjection scheme are switched on for 15° while the remaining sectors are also switched on for 15° to maintain equal width criterion. A zero current interval of $15^\circ = 833.34\ \mu$s is maintained using this scheme, which provides enough time for the thyristor to regain its blocking capability. As seen from Figure 6, each reinjection switch pair is switched on 7.5° before and switched off after 7.5° main bridge commutation occurs i.e S_{p1}/S_{n1} is switched on at -7.5° and switched off at 7.5°; S_{p0}/S_{n0} is switched on at 7.5° and switched off at 22.5°; S_{p2}/S_{n2} is switched on at 22.5° and switched off at 37.5° etc. Thus, controllable zero current durations are achieved.

3 Three-level thyristor based MLCR CSC

In Figure 4, the reinjection transformer is a single-phase two-winding transformer with transformer turns ratio of:

$$\frac{n_1}{n_0} = 1 \quad n_0 : \text{Primary turns and } n_1 : \text{Secondary turns of the reinjection transformer}$$

The primaries of the two reinjection transformers are connected across the DC bus through DC blocking capacitors (C). The DC current (I_{dc}) flows through the reinjection IGBTs, smoothing inductance L_{dc} and the load. It is chopped into AC waveforms in the secondary windings of the reinjection transformer with the help of reinjection switches (S_{p1}/S_{n1} etc). These currents are coupled to the reinjection transformer primary winding to form multilevel currents I_{j1} and I_{j2} which combine with I_{dc} to shape the DC bus currents I_1 and I_2 into multilevel waveforms. This reinjection circuit generates three current steps in I_1 and I_2. Two levels are generated due to reverse connected switches (S_{p1}/S_{n1} and S_{p2}/S_{n2}) and one additional level is obtained by firing S_{p0}/S_{n0} when I_{j1} and I_{j2} are both zero.

3.1 AC-side current waveforms

The theoretical analysis of the circuit shown in Figure 4 allows $I_a(\omega t)$ to be determined from the time domain components of the AC-side secondary currents $I_{aY}(\omega t)$ and $I_{caD}(\omega t)$. This gives:

$$I_a(\omega t) = \frac{1}{k_n}\left[I_{aY}(\omega t) + \sqrt{3}I_{caD}(\omega t)\right] \tag{2}$$

where k_n: interface transformer turns ratio. The corresponding current waveforms are shown in Figure 7 where the resulting current (I_a) THD_{3level} of 7.77% is obtained.

3.2 DC-side voltage waveforms

DC-side voltage waveforms (Figure 8) are time referenced with respect to the AC-side current waveform I_a (Figure 7). This is done to show that even with thyristor based converter, it is possible to switch the thyristors with a negative firing angle, as from Figure 8 it is clear that line current is leading the voltage.

Figure 7 Current waveforms for three-level thyristor based MLCR CSC with linear reinjection

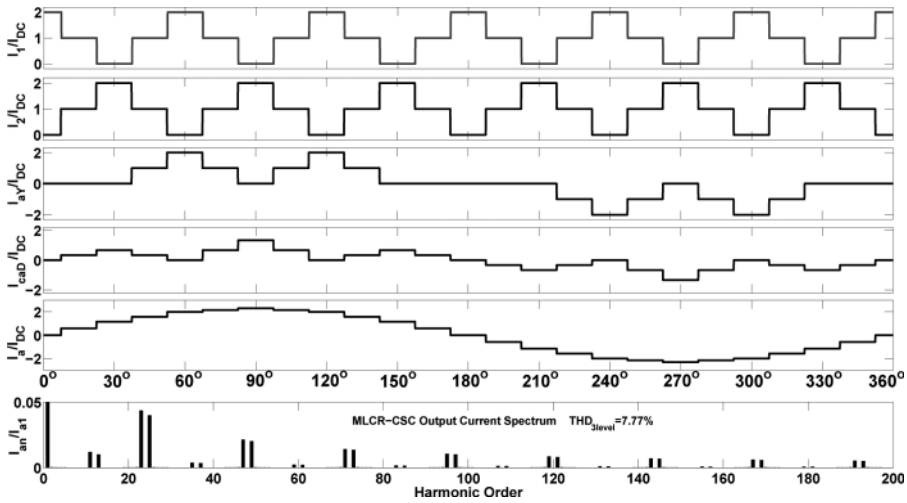

Figure 8 Theoretical DC voltage waveforms for three-level thyristor based MLCR CSC for $\alpha = -45^{\circ}$

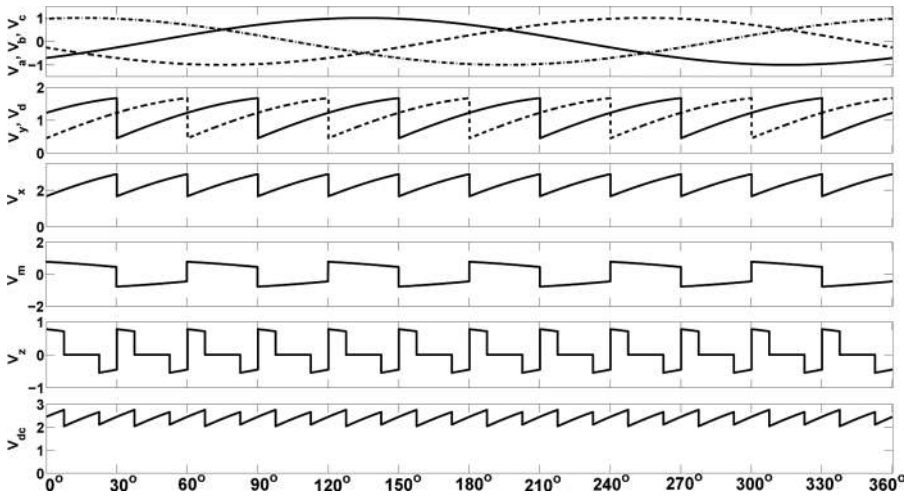

In Figure 8, the following voltages (all the voltages are plotted with respect to the peak phase source voltage (V_{pk})) are shown (c.f. Figure 4):

- the DC-side voltages across the individual 6-pulse bridges: V_y and V_d
- the DC-side voltages across the 12-pulse bridge: $V_x = V_y + V_d$
- the DC-side voltage across the secondary-side of the reinjection transformers: $V_m = V_{y_{ac}} - V_{d_{ac}} \approx V_y - V_d$

- the DC-side ripple voltage V_z: When the j^{th} pair of reinjection IGBT $S_{pj}/S_{nj}(j = 0, 1, 2)$ is switched on, then voltage V_z is:

$$V_z = \begin{cases} V_m, & 0 \leq \omega t \leq \frac{\pi}{24} \\ 0, & \frac{\pi}{24} \leq \omega t \leq \frac{\pi}{8} \\ -V_m, & \frac{\pi}{8} \leq \omega t \leq \frac{5\pi}{24} \\ 0, & \frac{5\pi}{24} \leq \omega t \leq \frac{7\pi}{24} \\ V_m, & \frac{7\pi}{24} \leq \omega t \leq \frac{\pi}{3} \end{cases} \tag{3}$$

- the output DC voltage: $V_{dc} = V_x + V_z \approx 3.39 \frac{V_{pk}}{k_n} \cos(\alpha)$.

Theoretical confirmation for the following can be inferred as:

- Thyristors can be switched on with negative firing angles.
- The possibility of switching thyristors with negative firing angle implies the self-commutation is achievable as commutation is independent of line voltage now.
- Line current THD is approximately halved for a 24-step AC-side current when compared to a 12-step line current. THD is approximately the same for different values of firing angle i.e. it does not depend on the value of firing angle unlike conventional thyristor based converters.

In a conventional thyristor based converter, the thyristor current does not commutate instantaneously from the outgoing thyristor to the incoming thyristor. There is a delay in transfer of current and this time is called the commutation angle. It is due to energy transfer between phase inductances and would be higher for a system with higher line inductances. Thus, line current always lag the phase voltage. However, with the help of the auxiliary reinjection bridge, commutation is avoided/reduced due to cancellation of thyristor current in the commutation instants which eliminates the overlap. Figure 9 shows the cancellation of currents in the commutation instants for thyristors Y1 and Y3 thereby elimination overlap.

Figure 9 Currents through thyristors Y1 and Y3 using PSCAD/EMTDC

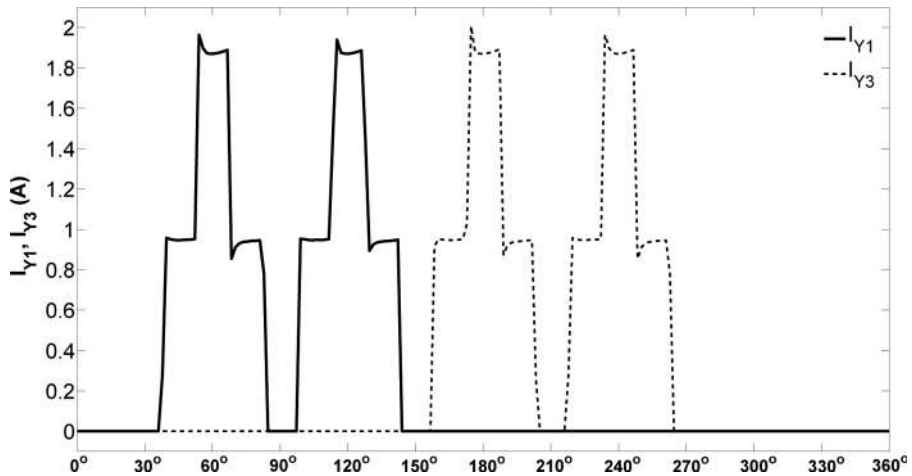

4 Experimental results

The successful operation of the prototype with output $V_{dc} = 96.3\,\text{V}$ and $I_{dc} = 0.94\,\text{A}$ using $\alpha = -45^\circ$ validates the concept of thyristor based MLCR CSC. For comparison with the theoretical waveforms, the experimental and theoretical waveforms are overlapped together.

4.1 Formation of I_{inj} using reinjection bridge

Table 1 shows the corresponding relationship between I_1 and I_2, I_{j1} and I_{j2} with the corresponding reinjection switch ON-state.

Table 1 Reinjection switching combination and three-level reinjection current

On-state switches	I_{j1}	I_1	I_{j2}	I_2
Sp1/Sn1	I_{dc}	$2I_{dc}$	$-I_{dc}$	0
Sp0/Sn0	0	I_{dc}	0	I_{dc}
Sp2/Sn2	$-I_{dc}$	0	I_{dc}	$2I_{dc}$

The 'chopping' of load current I_{dc} occurs with the help of the reinjection IGBTs. In Figure 10 $I_{Sp1} = I_{Sn1} = I_{dc}$ when $S_{p1}/\ S_{n1}$ are switched on. When $S_{p2}/\ S_{n2}$ are on, $I_{Sp2} = I_{Sn2} = I_{dc}$. For all other instants, $S_{p0}/\ S_{n0}$ are on when $I_{Sp0} = I_{Sn0} = I_{dc}$ and the reinjection bridge is bypassed. Figure 11 shows the reinjection currents I_{j1}, I_{j2} and I_{inj} on the primary side of the reinjection transformer.

Figure 10 I_{Sp1}, I_{Sp0} and I_{Sp2} experimental waveforms

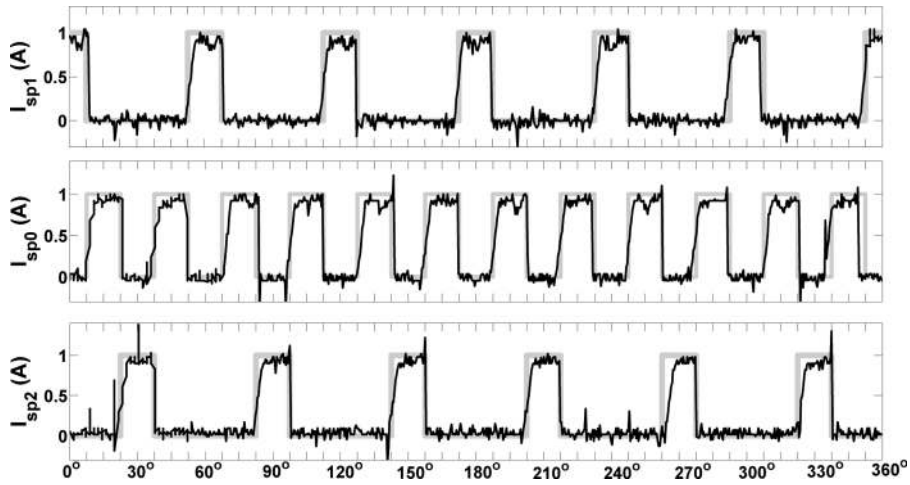

The experimental current waveforms are slightly distorted when compared to the theoretical waveforms. This is due to the RC snubber across the reinjection IGBT switches. The effect of RC snubber circuit was not considered while deriving the theoretical waveforms. RC snubber circuit is necessary to across the reinjection IGBT

in order to limit the rise in voltage across it due to the sudden interruption of current flowing through it.

Figure 11 I_{j1}, I_{j2} and I_{inj} experimental waveforms

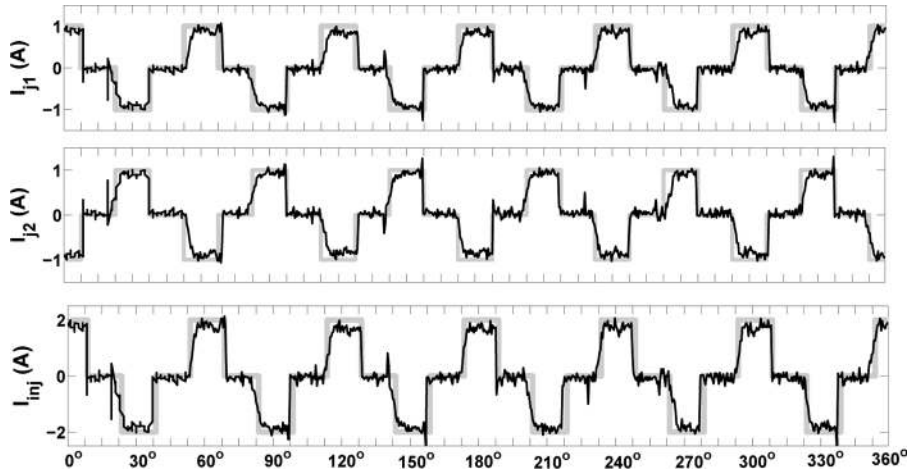

4.2 Modification of AC-side secondary currents due to I_{inj}

In Figure 2, the modification of AC-side secondary currents I_{aY} and I_{caD} due to I_{inj} is shown. Using the three-level I_{inj} obtained from the three-level reinjection bridge, the modified AC-side secondary line currents I_{aY} and I_{aD} are shown in Figure 12. In the experimental set-up, current I_{caD} is not available for measurement, hence the line current I_{aD} is shown instead.

Figure 12 Secondary-side line currents I_{aY} and I_{aD} experimental waveforms

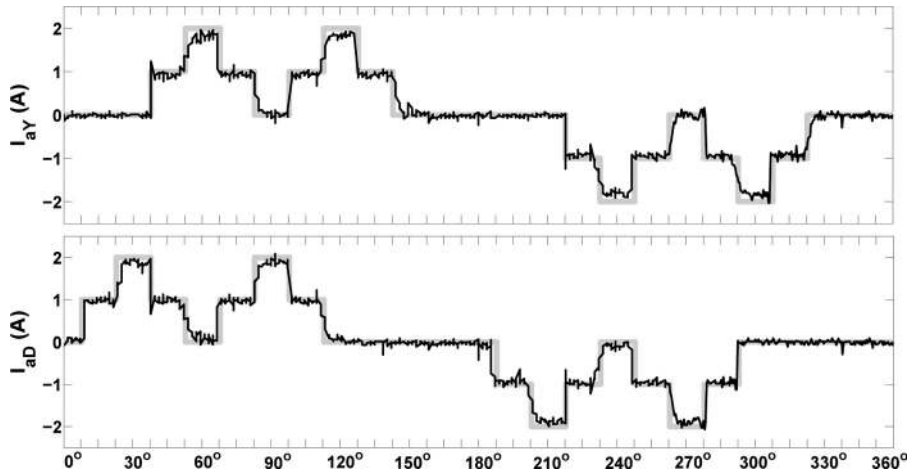

4.3 Formation of Stepped DC bus currents

The three-level reinjected current I_{inj} modifies the DC bus currents as shown in Figure 13. The DC bus currents are three-level waveforms as defined in Table 1 and are following the theoretical current wave-shape.

Figure 13 I_1 and I_2 experimental waveforms

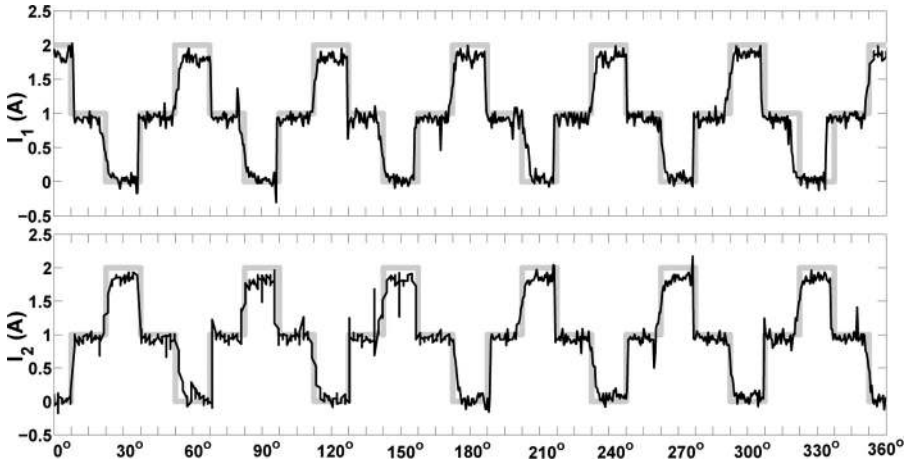

4.4 AC-side primary line current waveform

The modified primary-side line current I_a is shown in Figure 14. The modification of I_{aY} and I_{aD} also leads to modification of I_a (Equation 2). I_a is distorted when compared to the theoretical waveform but a 24-step waveform can be observed. This confirms the theory that line current THD reduction is possible by three-level current reinjection.

Figure 14 Primary-side line current I_a experimental waveform

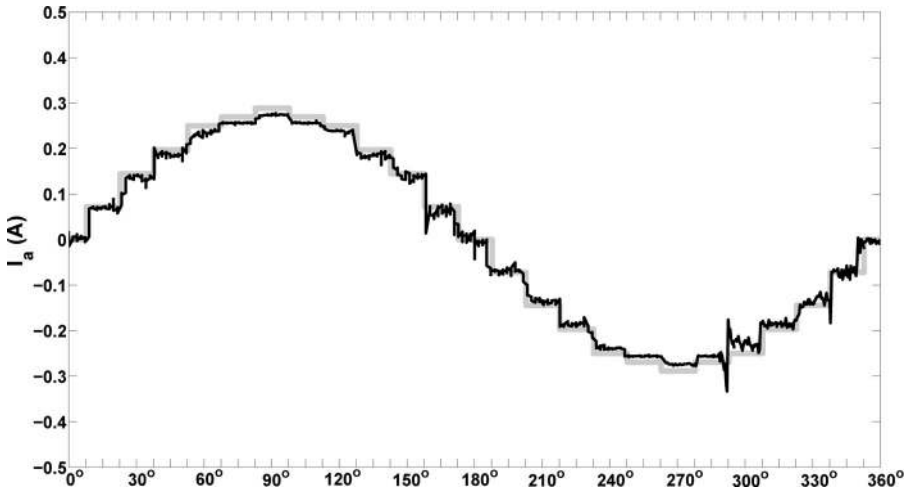

4.5 Modified main bridge thyristor current waveform

The modified current through thyristor Y1 I_{thyY1} is shown in Figure 15. I_{thyY1} starts to flow through Y1 when the reinjection circuit allows it to flow and similarly it can clamp I_{thyY1} to zero as well. It is clearly observed from this waveform that I_{thyY1} is clamped to zero when Y1 is fired (15° before I_{thyY1} flows). Thus, current flow through thyristor can be controlled independently using the reinjection bridge. This demonstrates the ability to operate thyristors as self-commutated switches.

Figure 15 I_{Y1} experimental waveform

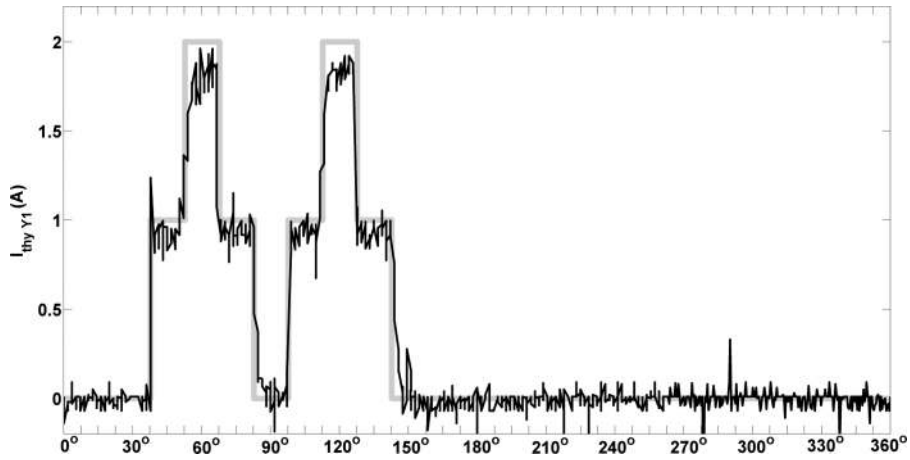

4.6 Y-Y and Y-D connected bridge DC voltage waveforms

The DC voltage waveform for both Y-Y and Y-D connected 6-pulse bridges are shown in Figure 16. **DC-side voltage waveforms (Figure 16) are time referenced with respect to the AC-side current waveform I_a (Figure 14)**.

Figure 16 V_y and V_d experimental waveform (see online version for colours)

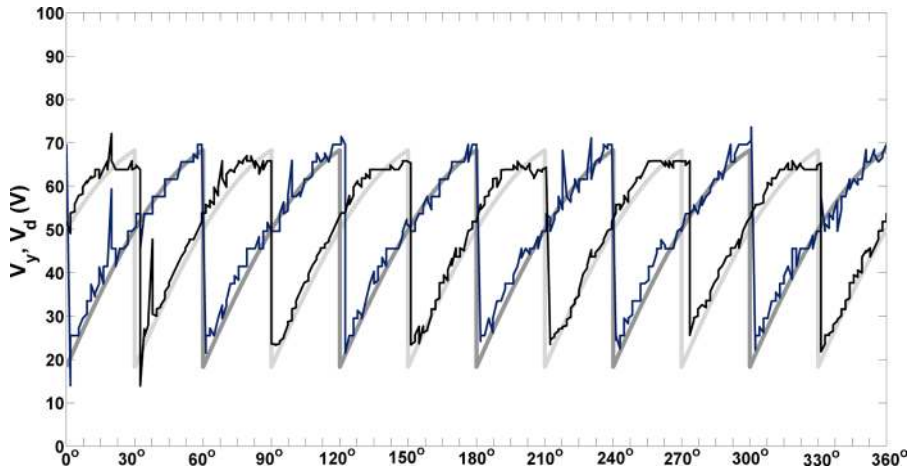

4.7 Output DC voltage waveforms

The DC voltage waveform V_{dc} is shown in Figure 17. V_{dc} has 24 pulses which implies that ripple voltage is getting added to V_x giving it 24-pulse characteristics. However, small amount of $\frac{dv}{dt}$ can be observed in V_{dc}, mostly around Y-D bridge commutation instants.

Figure 17 V_{dc} experimental waveform

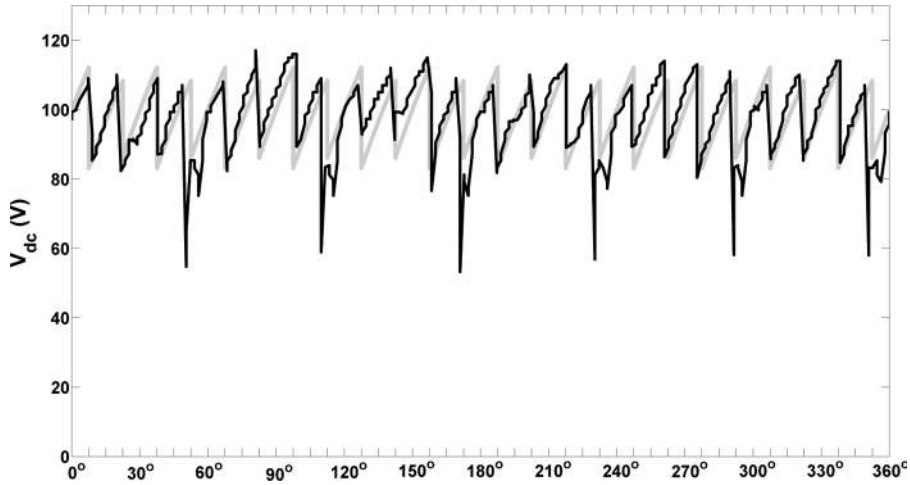

4.8 Probable causes for distortion – voltage spikes

Two possible causes of deviation from ideal MLCR output characteristics can be identified:

- snubber circuit design
- implementation of dead time in the reinjection circuit.

4.8.1 Snubber circuit design

When a power electronic converter stresses a power semiconductor device beyond its ratings, there are two ways of relieving the problem.

- replace device by one whose ratings exceed the stresses
- a snubber circuit can be added to the basic device to reduce the stresses to safe levels.

A trial and error method which used the basic assumption that IGBT current change linearly in time with a constant $\frac{di}{dt}$, was used to determine the snubber component values. However, actually $\frac{di}{dt}$ which may be different at turn-on and turn-off, is affected by the addition of the snubber circuit. This assumption provides the basis for a

simple design procedure for a laboratory prototype. The final design will be somewhat different depending on what is revealed by laboratory measurements on the actual prototype circuit.

The final choice will be a trade-off between cost and availability of the semiconductor device with the required electrical ratings compared to the cost and the additional complexity of using a snubber circuit. The presence of stray inductances results in an over-voltage. For MLCR CSC applications, this over-voltage will be a function of the leakage inductances of the reinjection transformer. Hence, a reinjection transformer with low leakage inductance is critical in determining the reinjection switch rating. An approximate way to determine the leakage reactance is to apply a short-circuit across the secondary. Thus from the Short Circuit test of the reinjection transformer, the leakage reactance is calculated to be 1.242 Ω for a transformer with base impedance of 160 Ω ((400V)^2/1kVA). Therefore the leakage reactance = 3.95 mH. This energy now needs to be dissipated in the snubber.

When the RCD snubber is used as a voltage clamping circuit they are used to clip the voltage spikes that occurs because of the resonance of the leakage inductance with the output capacitance of the reinjection IGBT. IGBTs have a maximum V_{ce} voltage which should not be exceeded. The clamp can be designed so that this maximum voltage is never exceeded. The value of the capacitor can be determined by selecting how much voltage change can occur. The ripple voltage is denoted as dV. The value of capacitor can be determined as:

$$\frac{1}{2}CV^2 + \frac{1}{2}LI^2 = \frac{1}{2}C(V + dV)^2 \tag{4}$$

where $\frac{1}{2}CV^2$: is the initial energy stored in the capacitor, $\frac{1}{2}LI^2$: is inductor energy and $\frac{1}{2}C(V + dV)^2$: is the fully charged capacitor. On solving (4), the snubber value is:

$$C = \frac{LI^2}{dV(dV + 2V)} \tag{5}$$

From calculations – maximum voltage appearing across $IGBT = 36.72$ V, maximum IGBT current = 1 A, calculated leakage inductance $L_{lk} = 3.95$ mH, assumed ripple voltage = 40 V, the snubber capacitance = 0.87 μF. Resistance is chosen to be less than 166.66 μs ($\frac{1}{10}^{th}$ of switching time of S_{p0}/S_{n0} reinjection IGBT pair). Hence, $\tau_{RC} = 50\,\mu$s, where snubber resistance = 57 Ω/2W.

Considering the leakage reactance, a much higher snubber capacitance is needed than what was used by the trial and error method with McMurray's equation. But when snubber capacitance = 1 μF is used, improvement in voltage waveforms was evident while the current waveforms were highly distorted. A different snubber capacitor value to the one calculated using McMurray's equation improved the voltage waveform. This was due to a different mechanism causing the voltage spike (as elaborated on in the next section) than the typical inductive energy in the transformer leakage reactance having to be controlled by the snubber circuit at turn-off.

4.8.2 Dead time in the reinjection circuit

Initially, there was no dead time implemented in the experimental setup. However, on powering up the MLCR CSC circuit, there was a short circuit which was observed

with blown IGBT switches. After inspection it was decided to have a small dead time between the reinjection circuit to alleviate the problem. However, getting a fixed dead time was a problem with analog components because of component tolerance variations, hence a dead time of 10μs was decided upon. This value was chosen as it encompassed all the variation in the switching pulse edges for the reinjection switches.

However, implementing dead time caused voltage spikes. Each time S_{p0}/S_{n0} (in PSCAD/EMTDC simulation, the switches overlap and no dead time is implemented) is opened, I_{dc} is interrupted, causing a voltage spike across load inductance L_{dc}. From Figure 17, it can be seen that there is variation in the sizes of the spikes, yet they repeat in a pattern. This can be attributed to the variation in the dead-time due to component tolerances. Hence, the inductive energy in the load is a major contributor to the voltage spikes. The issue of enabling the overlapping of switching waveforms without destroying the IGBTs to improve the voltage waveform is an issue which needs to be addressed in future. Another way of controlling the voltage spikes would be the addition of a freewheeling diode to carry I_{dc} when all the reinjection switches are open or by implementing a clamp circuit across the load.

5 Conclusion

Technical concerns which have been addressed in this paper are as follows:

- The modification of the current through the main bridge thyristors shows that self-commutation for thyristors can be achieved using the reinjection bridge despite finite turn off time of thyristors.
- As the reinjection IGBTs can be turned off at will, the main bridge thyristor can be switched on at a negative firing angle. This provides the thyristor main bridge to reactive power control capability.
- Commutation overlap is avoided due to current clamping to zero provided by the reinjection bridge.
- The three-level MLCR concept provides 24-pulse operation of a 12-pulse thyristor converter. This improves the harmonic content of current and voltage on both the AC and DC-side. Size reduction of the smoothing inductor due to a low harmonic content on the DC-side is possible.
- Size reduction of reinjection transformer is possible due to operation at 300 Hz. These transformers apply a low voltage to reinjection switches.

The investigation of the performance of the three-level MLCR CSC under steady-state conditions showed a good agreement between the experimental and the theoretical current waveforms. From experimental results, it is observed that the deviation of the actual waveforms from the theoretical waveforms is mainly due the inductive energy in the load which is a major contributor to the voltage spikes. Two ways of controlling the voltage spikes would be the addition of a freewheeling diode to carry I_{dc} when all the reinjection switches are open or by implementing a clamp circuit across the load.

References

Arrillaga, J., Liu, Y.H., Crimp, C.S. and Villablanca, M. (1993) 'Harmonic elimination by DC ripple reinjection in generator-converter units operating at variable speeds', *Proc. Inst. Elec. Eng. (IEE) Gen., Trans. and Dist.*, Vol. 140, No. 1, pp.57–64.

Arrillaga, J., Liu, Y.H., Perera, L.B. and Watson, N.R. (2006) 'A current reinjection scheme that adds self commutation and pulse multiplication to the thyristor converter', *IEEE Trans. Power Del.*, Vol. 21, No. 3, pp.1593–1599.

Baird, J.F. and Arrillaga, J. (1980) 'Harmonic reduction in DC-ripple reinjection', *IEE Proc. Part-C*, Vol. 127, pp.294–303.

Gairola, S. and Singh, B. (2011) 'Power quality improvements employing multipulse full-wave AC-DC converters', *Int. J. of Power Electronics*, Vol. 3, No. 3, pp.240–298.

Kimbark, E.W. (1996) *Direct Current Transmission*, 1st ed., Vol. 1, John-Wiley and Sons Inc., Toronto, Canada (Ch. 3).

Liu, Y.H. (2003) *Multi-Level Voltage and Current Reinjection AC-DC Conversion, PhD thesis*, Electrical and Computer Engineering Department, University of Canterbury, New Zealand.

Liu, Y.H., Arrillaga, J. and Watson, N.R. (2008) 'Reinjection concept: a new option for large power and high-quality AC/DC conversion', *IET Power Elec.*, Vol. 1, No. 1, pp.4–13.

Liu, Y.H., Watson, N.R., Arrillaga, J. and Perera, L.B. (2006) 'Multi-level current reinjection CSC for STATCOM application', *Proc. IEEE Int. Conf. Power Sys Tech (POWERCON)*, Chongqing, China, 22–26 October, pp.1–5.

Liu, Y.H., Perera, L.B., Arrillaga, J. and Watson, N.R. (2007a) 'A back to back HVdc link with multilevel current reinjection converters', *IEEE Trans. Power Del.*, Vol. 22, No. 3, pp.1904–1909.

Liu, Y.H., Perera, L.B., Arrillaga, J. and Watson, N.R. (2007b) 'Application of the multilevel current reinjection concept to HVDC transmission', *IET Gen. Trans. Dist.*, Vol. 1, No. 3, pp.399–404.

Mohan, D.M., Singh, B. and Panigrahi, B.K. (2009) 'Power quality improvement in HVDC systems using 18-pulse voltage source converter', *Int. J. of Power Electronics*, Vol. 1, No. 3, pp.333–346.

Murray, N.J., Arrillaga, J., Watson, N.R. and Liu, Y.H. (2009) 'Four quadrant multilevel current source power conditioning for superconductive magnetic energy storage', *Proc. Australasian Universities Power Engineering Conference (AUPEC)*, Adelaide, SA, 27–30 September, pp.1–5.

Paice, D.A. (1996) *Power Electronic Converter Harmonics: Multipulse Methods for Clean Power*, IEEE Press, New York, NY, USA.

Rodriguez, J., Lai, J.S. and Peng, F.Z. (2002) 'Multilevel inverters: a survey of topologies, controls, and applications', *IEEE Trans. Ind. Electron.*, Vol. 49, No. 4, pp.724–738.

Villablanca, M.E., Arias, M. and Acevedo, C. (2002) 'High-pulse series converters for HVDC systems', *IEEE Trans. Power Del.*, Vol. 16, No. 4, pp.766–774.

Appendix: experimental parameters

Source specification

- Voltage rating: 400 V @ 50 Hz
- Source impedance: $0.058\,\Omega + 4.065\,\text{mH}$

Interface transformer

- Type: 3-phase, 3-winding @ 50 Hz
- Power rating: 2 kVA
- Voltage rating: 400 V: 50/50 V

Reinjection transformer

- Type: 1-phase, 2-winding @ 300 Hz
- Measured impedance: $R_{eq} = 3.8\Omega$, $X_{eq} = 1.2\Omega$
- Power rating: 1 kVA
- Voltage rating: 400 V: 400 V

Load specification

- Measured load resistance: 106 Ω
- Measured load inductance: 593 mH

Firing angle

- α: -45°